JOURNAL OF MATERIALS SCIENCE 8 (1973) 883-892

# Properties of alloys on the tie-line between the copper-CuZrGe pseudo-binary eutectic and the copper-$Cu_5Zr$ eutectic

A. J. PERRY, A. R. NICOLL*
*Brown Boveri Research Centre, CH-5401 Baden, Switzerland*

The electrical conductivity of copper-CuZrSi alloys is shown to be improved by making them zirconium-rich; however, the volume fraction of the strengthening phase is thereby reduced. To counteract the loss of strength, the isotypic copper-CuZrGe system with its higher volume fraction of second phase was studied. The UTS was found to be higher, the high elongation to failure being retained. To study the variation of conductivity, alloys on the tie-line to the copper-$Cu_5Zr$ eutectic were investigated. It was found that conductivity values which are proportional to the volume fraction of copper can be achieved. The tensile properties follow a law-of-mixtures pattern as control of failure passes from the weaker, ductile copper-CuZrGe eutectic to the stronger, much less ductile ternary eutectic. This ternary eutectic is found to be close to the copper-$Cu_5Zr$ eutectic; the tensile properties of the two eutectics are similar, being controlled by the $Cu_5Zr$ phase which is present in both to about the same volume fraction.

## 1. Introduction

This paper describes the properties of unidirectionally solidified (UDS) alloys lying on the tie-line between the copper-CuZrGe pseudo-binary eutectic and the copper-$Cu_5Zr$ eutectic. The work followed on from our previous studies of UDS copper-base eutectics.

The tensile properties of the UDS copper-CuZr*Si* pseudo-binary eutectic were measured previously [1]: we found an ultimate tensile stress (UTS) of about 42 kg $mm^{-2}$ and a total elongation-to-fracture of some 8 to 10%. This was achieved using a high temperature gradient at the solid-liquid interface to suppress cell formation, which deleteriously affects the UTS, though not the elongation. The tensile curves were observed to display the characteristics of a Lüders band propagation on yielding. The study has since been extended to include the electrical conductivity, which was found to be rather poor (about 35 $\mu\Omega^{-1}$ $m^{-1}$ or some 60% IACS†) although the volume fraction of the CuZrSi phase in the eutectic is only 9.2 vol %. As shown below (Section 3) the conductivity can be improved by making the alloys zirconium-rich though they then become weaker as the volume fraction of the CuZrSi phase is reduced. If it is reduced too far then it will become insufficient for fibre-strengthening, which requires [3] a minimum critical volume fraction. It may be possible to counteract this tendency by substituting the isotypic copper-CuZr*Ge* pseudo-binary eutectic where the volume fraction is greater at about 10.4 vol % (as calculated from the theoretical density based on the lattice parameters [4]).

We show here (Section 4) that this substitution is acceptable because the copper-CuZrGe eutectic (hereafter referred to as $E_1$) has properties similar to the copper-CuZrSi eutectic: firstly, Lüders band-type yielding with a high elongation-to-fracture, and secondly, poor electrical conductivity which can be improved by making the alloys zirconium-rich (Section 6). We then went on to study the variation of conductivity and tensile properties in alloys more zirconium-

*Now at: Brown Boveri Zentrales Forschungslaboratorium, Postfach 20b, D-6900 Heidelberg 1, Germany.
†IACS: the International Annealed Copper Standard is a reference value for the conductivity of copper quoted as 58 $\mu\Omega^{-1}$ $m^{-1}$ at 20 °C, high purity copper is normally [2] about 59.7 $\mu\Omega^{-1}$ $m^{-1}$ or 102.9% IACS; our OFHC copper starting material was measured at 59.2 $\mu\Omega^{-1}$ $m^{-1}$ (102% IACS) at 20°C.

rich than $E_1$ in order to optimize them. The alloys studied were confined to the tie-line between $E_1$ and the copper-$Cu_5Zr$ eutectic (referred to as $E_2$) as shown in Fig. 1. This was done because the phase space bounded by copper, $E_1$ and $E_2$ could not contain the ternary eutectic $E_t$; hence the present alloys may contain dendritic copper but should not contain any primary CuZrGe or $Cu_5Zr$, which could lead to premature tensile failure.

From preliminary studies (Section 5) it appeared that the eutectics $E_t$ and $E_2$ nearly coincide. This was fortunate because it allowed a further aspect to be studied. This concerned the tensile properties of alloys on the $E_1$—$E_2$ tie-line. They represent a series of composite materials comprising $E_1$ and $E_t$ (possibly with dendritic copper also). $E_t$ is a copper-$Cu_5Zr$-CuZrGe eutectic mixture whilst $E_2$ is copper-$Cu_5Zr$. This latter phase is the primary load carrier in both and its volume fraction is about the same in both of them. The $E_t$ therefore, as found with $E_2$ [5], should have high strength but poor elongation-to-fracture characteristics in contrast to the weaker, ductile $E_1$. The system thus parallels the copper-tungsten case [3, 6] and we expect this classical form of tensile strength-volume fraction relation to be seen here.

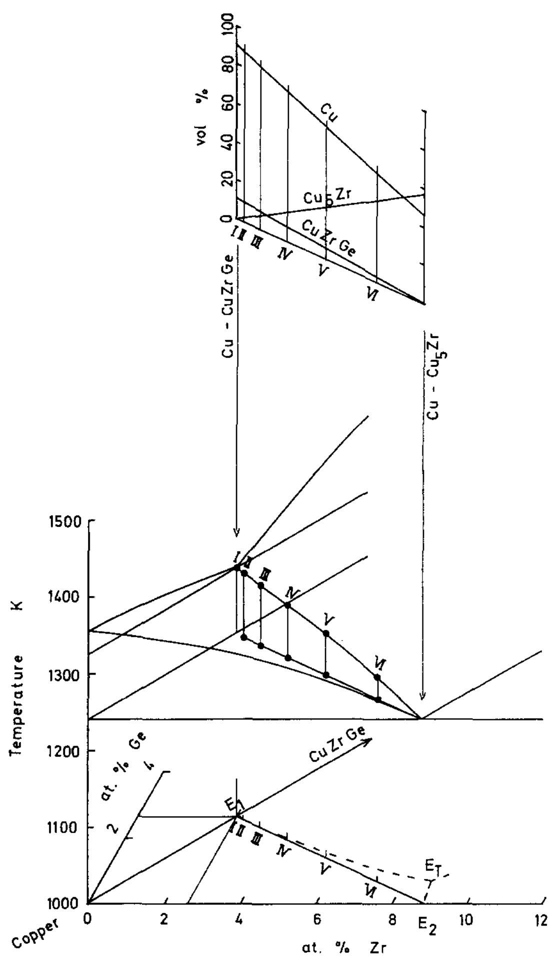


*Figure 1* A partial equilibrium diagram of the copper-zirconium-germanium system showing the tie-line between the copper-CuZrGe and copper-$Cu_5Zr$ eutectics ($E_1$ and $E_2$ respectively) and indicating the compositions of the present alloys I-VI. Also included are the thermal analysis results from these alloys and (inset) the volume fractions of the phases present in them. The location of the ternary eutectic $E_t$, as determined by EMA, and the probable positions of the eutectic troughs are included.

## 2. Experimental procedure

The alloys made in the present study were based on copper and zirconium of 99.93 and 99.99% purity, respectively, and semi-conductor-pure silicon or germanium. They were of the nominal compositions I-VI indicated in Fig. 1 and XI-XIV in Fig. 2. Also shown for the former are

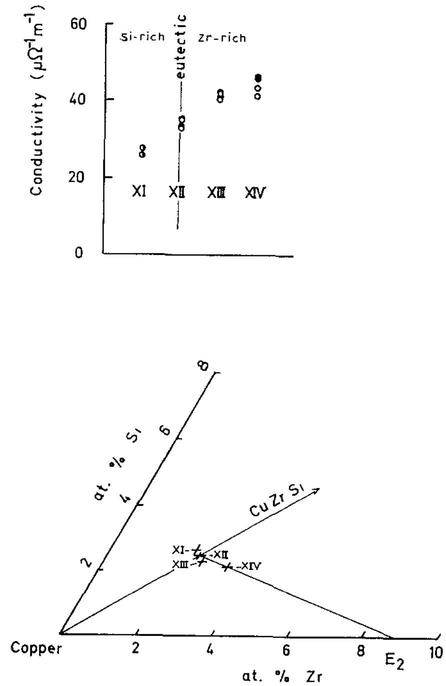


*Figure 2* The constitution and electrical conductivity of the present copper-CuZrSi alloys XI-XIV. The conductivity was determined at 20°C both before and after (open and filled symbols) a heat-treatment of 12 h at 773 K followed by furnace cooling.

the theoretical volume fractions of each phase based on the known density 8.96 g $cm^{-3}$ of copper [7], the density of the CuZrGe phase (7.81 g $cm^{-3}$) calculated from the lattice parameters [4] and the density 7.86 g $cm^{-3}$ of the $Cu_5Zr$ phase derived previously [5].

The location of the $E_1$ eutectic was determined as 2.6 at. % zirconium and 2.6 at. % germanium at a temperature of 1328 K (1055° C). The alloys II-VI on the $E_1$—$E_2$ tie-line were also subjected to differential thermal analysis (DTA) and the results are included in Fig. 1. The ternary eutectic temperature is 1246K (973° C) which is about the same within experimental error as (but must in fact be less than) that of $E_2$ [8].

The experimental procedure for unidirectional solidification (UDS) was identically the same as used in the previous studies [1, 5]. After UDS the majority of specimens was subjected to a thermal treatment for varying periods of time at 773K, all specimens being furnace-cooled. The conductivity and tensile properties were determined as before. Subsequently the specimens were sectioned for optical microscopy and the total volume fraction of intermetallic phases was checked using a Quantimet B through the courtesy of Dr P. J. Goodhew at the University of Surrey. These determinations checked well with the theoretical volume fractions given in Fig. 1.

## 3. Conductivity of copper-CuZrSi alloys

As remarked in the Introduction, the conductivity of the pseudobinary eutectic is typically only about 60% IACS although the volume fraction of copper there is 90.8 %. Alloys to the silicon- and zirconium-rich sides have lower and higher conductivity respectively, as shown in Fig. 2. Alloys of composition XIII and XIV (Fig. 2) both contain areas of a fine, second eutectic-type phase as shown in the as-cast structure of XIII given in Fig. 3. Thus the conductivity is better in alloys zirconium-rich of the pseudobinary copper-CuZrSi line. Attributing the low conductivity to solid solubility of the CuZrSi phase in copper, the increase in conductivity shown in Fig. 2 must reflect a change in the nature of the copper solid solution (i.e., the copper solvus). The solubility would appear to decrease in moving the alloy composition towards $E_2$, at which limit the solubility of zirconium in copper is quite small [9].

The nature of the second eutectic-type phase in alloys XIII and XIV was investigated by

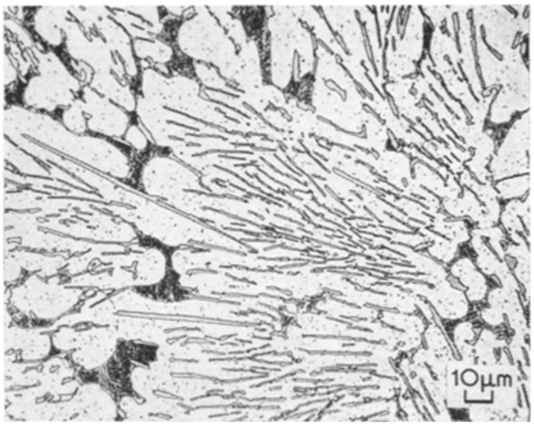


*Figure 3* Etched microstructure of the as-cast copper-zirconium-silicon alloy XIII showing coarse copper-CuZrSi eutectic and areas of a fine ternary eutectic.

electron microprobe analyser (EMA) and shown to be very closely that of the $E_2$ eutectic but with a negligible (i.e. indeterminate but less than 0.05 %) amount of silicon in addition.

## 4. Properties of the UDS copper-CuZrGe eutectic

Moving the alloy composition away from the copper-CuZrSi eutectic point by making it zirconium-rich decreases the volume fraction of the strengthening CuZrSi phase. Therefore, to avoid the onset of fibre-weakening caused by a subcritical volume fraction [3], the properties of the isotypic copper-CuZrGe system have been looked into. The volume fraction of CuZrGe in the eutectic is about 10.4 vol % as opposed to the 9.2 vol % in the earlier one.

The properties of the as-grown $E_1$ eutectic samples are indeed quite similar to the earlier ones [1] and are included in Fig. 8: the conductivity was still about 35 $\mu\Omega^{-1}$ $m^{-1}$ (60% IACS) and taken to indicate solubility of the CuZrGe phase in copper as before. The microstructure also showed cells with coarsening at the boundaries (Fig. 4) under the same growth conditions. Their effect on the tensile properties was the same in the growth rate range (1.6 to 16 × $10^{-2}$ mm $sec^{-1}$) studied: the UTS was independent of growth rate, but somewhat higher at 36 kg $mm^{-2}$ with an elongation-to-fracture of some 7%. The copper-CuZrSi eutectic [1] possessed a UTS of 32 kg $mm^{-2}$ but this could be increased to 42 kg $mm^{-2}$ by suppressing cell formation during growth through a high temperature gradient at the

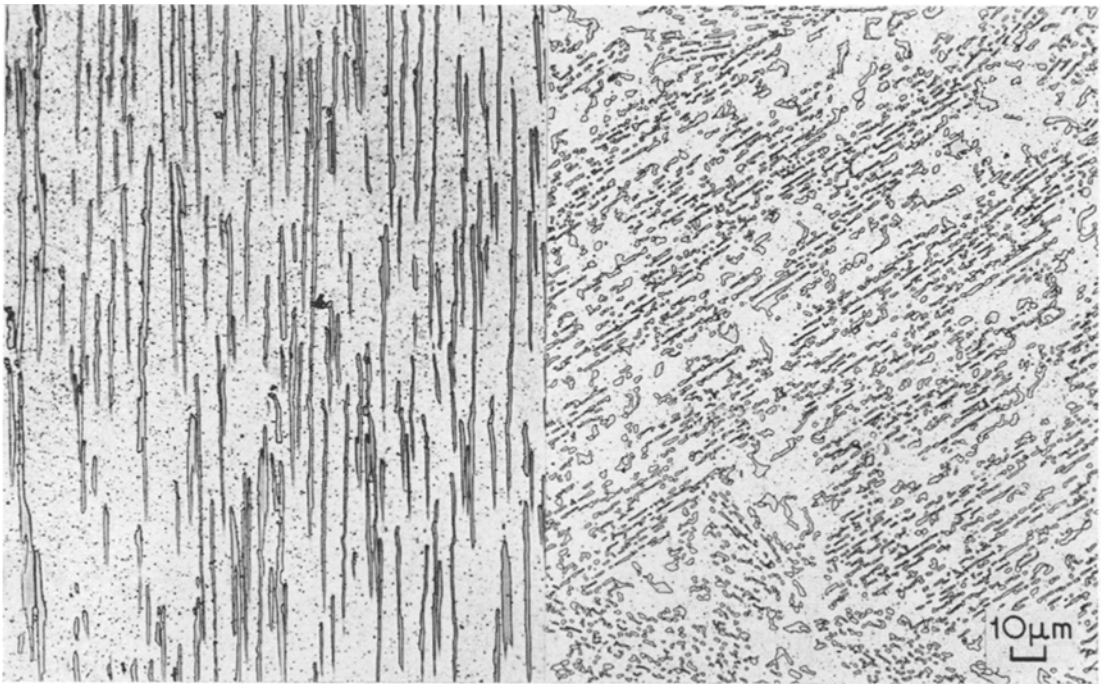


*Figure 4* Etched longitudinal and transverse sections of a UDS copper-CuZrGe eutectic (alloy I) grown at $16.0 \times 10^{-2}$ mm sec$^{-1}$ showing cells of the blade-like eutectic.

solid-liquid interface. If this were done in the present alloy, then (allowing for the greater volume fraction of CuZrGe) a level of 46 kg mm$^{-2}$ should be attainable.

Most of the tensile curves showed the Lüders band type of behaviour (Fig. 5a) as before, and again the local nature of the yielding was demonstrated by an attached extensometer whose record is included in Fig. 5a. It was found that some specimens showed serrated yielding to a greater or lesser degree – an extreme example is shown in Fig. 5b, curve a. In such cases the intercellular CuZrGe phase was found to be cracked (Fig. 6a) throughout the gauge length. The extent of cracking appeared to be related to the degree of serration; a cautionary note is in order: our metallography was confined to one longitudinal and two transverse sections, making any correlation uncertain because the sections may not have been typical. Presumably the CuZrGe phase cracks locally as the Lüders front passes through, because samples which failed prematurely just after the yield drop, seldom showed such cracks. In addition, mechanical twinning was seen as shown in Fig. 6b (and also in prematurely failed samples), sometimes with locally formed secondary twins, as shown in Fig. 6c. Only one sample (of alloy III) showed extensive twinning (Fig. 6d), but no cracking. In this instance, the tensile curve was smooth (Fig. 5b, curve b), indicating that the serrations are not due to twinning but are only associated with the cracking of the intercellular CuZrGe phase.

## 5. Microstructure of alloys on the $E_1$ — $E_2$ tie-line

The microstructure of the as-cast alloys II and III is similar to that of the copper-CuZrSi alloy XIII which is shown in Fig. 3. The second eutectic was again analysed by EMA and found to be of composition very close to $E_2$, i.e., containing additionally about 0.45 at. % germanium (Fig. 1). The microstructure of the alloys after UDS is typified by Fig. 7a. The cell structure found in alloy I (Fig. 4) is still evident but the ternary eutectic regions have become degraded to give mainly the $Cu_5Zr$ phase (and including little free copper) associated with CuZrGe in the cell walls.

The as-cast alloys IV to VI are microstructurally similar to their cross-sections *after UDS*, which are shown in Figs. 7b and c. Areas of $E_t$ are seen together with primary copper dendrites

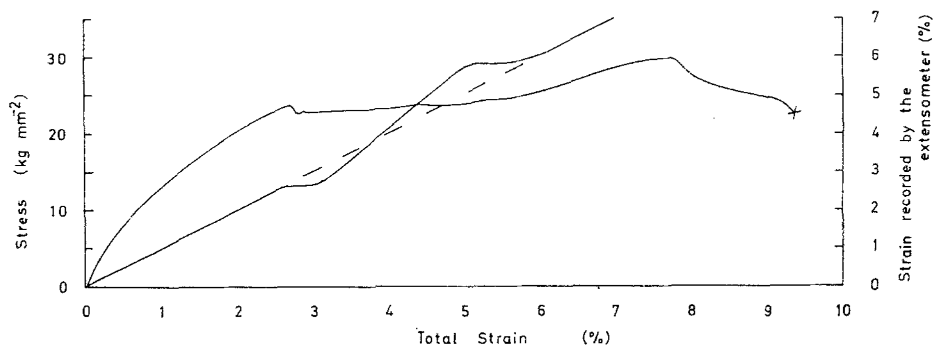


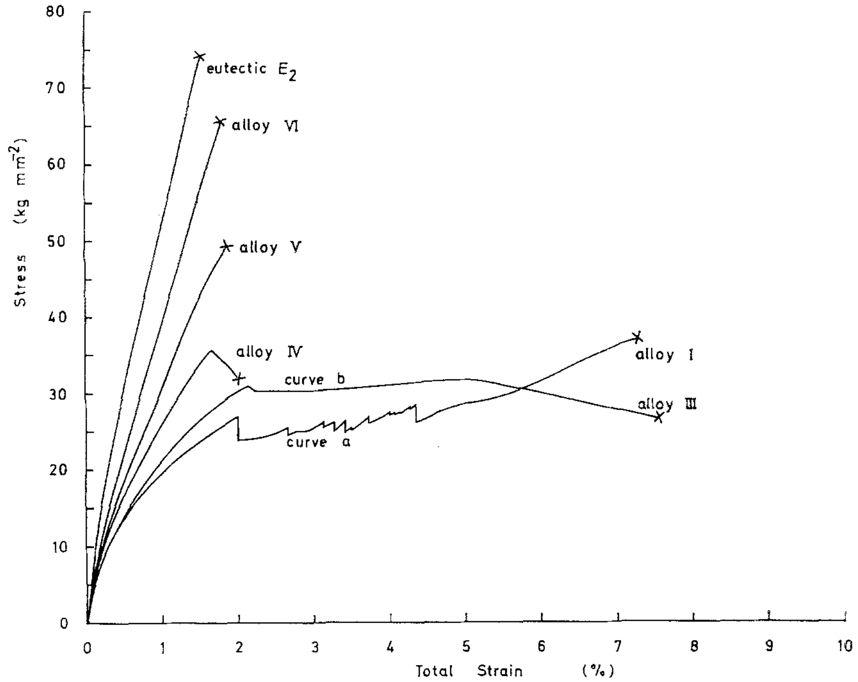


*Figure 5* (a) The stress-strain curve of a copper-CuZrGe eutectic (alloy I) sample grown at $5.3 \times 10^{-2}$ mm sec$^{-1}$ together with the strain recorded (right hand ordinate) by an attached strain gauge extensometer. Its gauge length was 10 mm as compared with 20 mm of the specimen. (b) Stress-strain curves of alloys I-VI all grown at $5.3 \times 10^{-2}$ mm sec$^{-1}$. Curve *a* shows an extreme example of the serrated yielding associated with cracking (Fig. 6a) of the intercellular CuZrGe phase. An example of smooth yield behaviour found in alloy III is shown in curve *b* where only twinning (Fig. 6d) but no cracking was found.

and angular CuZrGe. In these alloys, which are slightly copper-rich with respect to the $E_1$—$E_t$ trough, $E_1$ seems to become progressively degraded so that its copper grows on to the primary dendritic copper and rejects the CuZrGe, which then grows independently. In alloy VI (Fig. 7c), the completely rejected CuZrGe is seen embedded in the ternary eutectic, in contrast to alloy IV (Fig. 7b) where some lies between areas of $E_t$ and undegraded $E_1$. The ternary eutectic microstructure was found to be very similar to that of $E_2$ [5] consisting of copper and $Cu_5Zr$ lamellae with fine particles of CuZrGe randomly dispersed throughout both the other phases. It is worth remarking at this point that the proximity of $E_t$ and $E_2$ and the similarity of their microstructures are the origin for the last

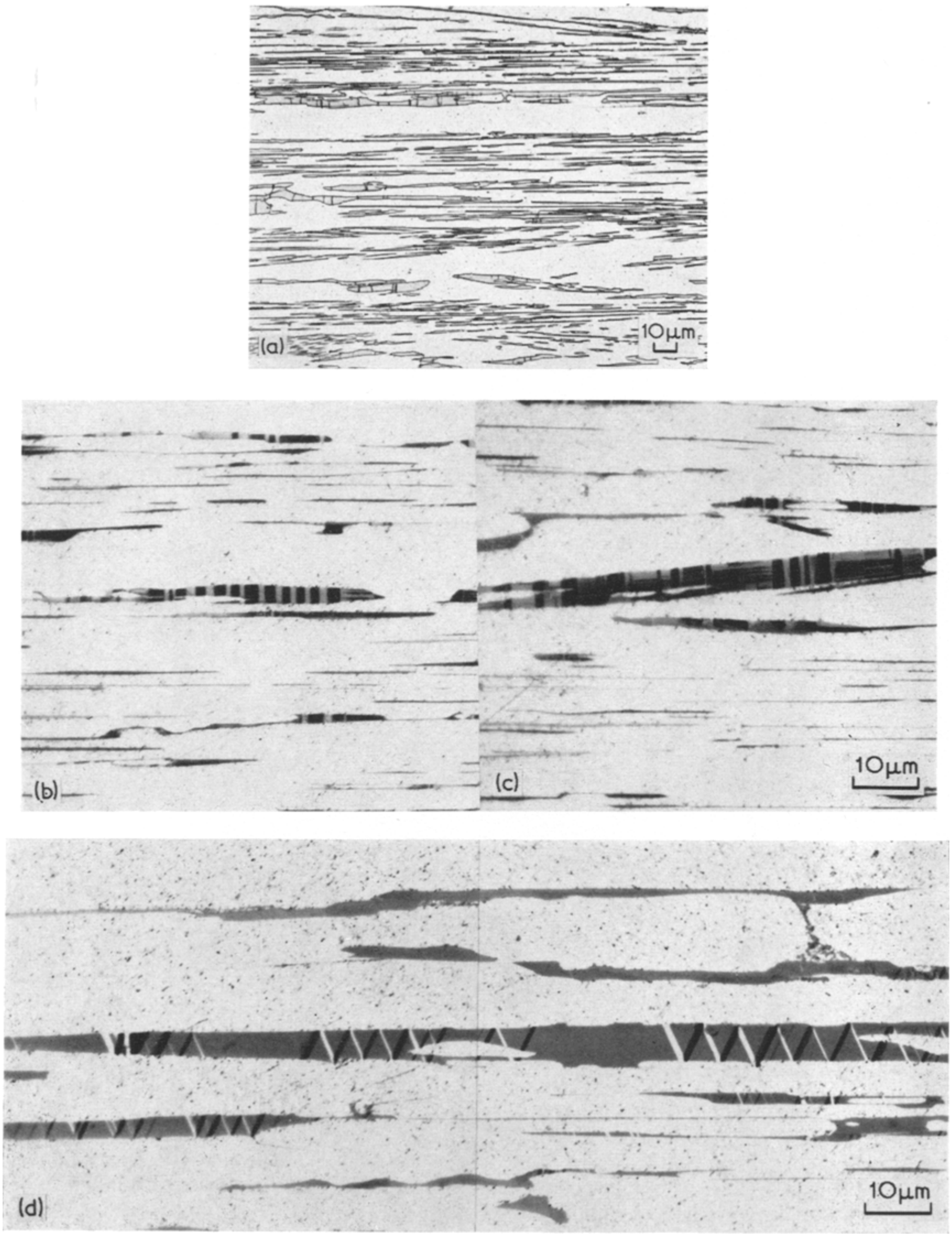


*Figure 6* Longitudinal micrographs taken from sectioned and etched samples of alloy I after tensile testing showing: (a) cracking of the intercellular CuZrGe phase (sample grown at $16.0 \times 10^{-2}$ mm $sec^{-1}$), (b) primary and, in the same sample, (c) local secondary twinning, under polarized light (sample grown at $5.3 \times 10^{-2}$ mm $sec^{-1}$). In (d) a longitudinal section of alloy III is shown which exhibited smooth yield behaviour (Fig. 5b, curve *b*) showing twinning under polarized light.

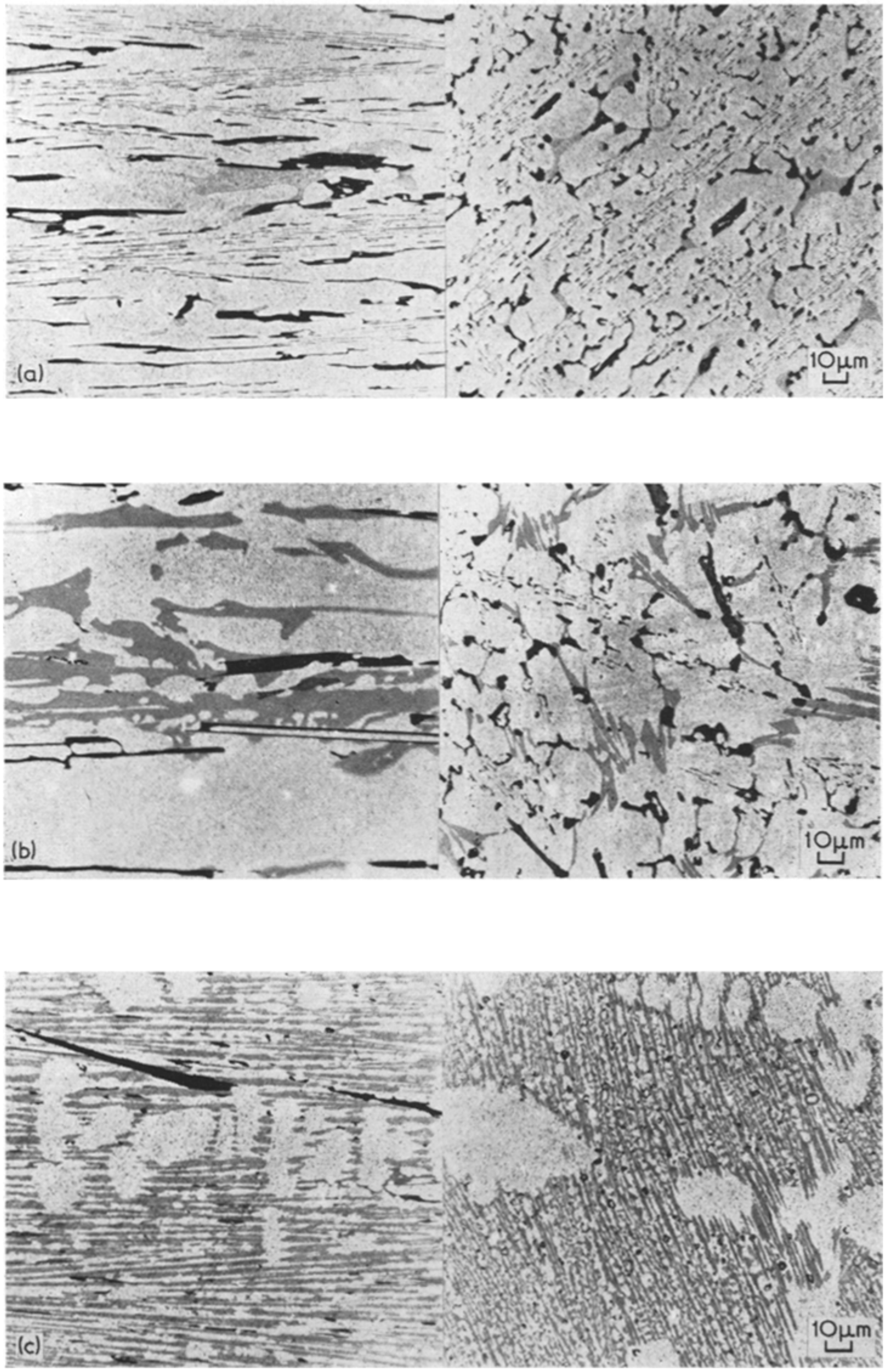


*Figure 7* Longitudinal and transverse microsections of (a) alloy III, (b) alloy IV and (c) alloy VI grown at 1.6, 5.3 and 16.0 $\times$ $10^{-2}$ mm $sec^{-1}$ respectively. Under polarized light the CuZrGe phase appears dark and it can be seen in very fine form in the ternary eutectic in (b). It is also apparent in (c) together with an apparently primary form resulting from degradation of the copper-CuZrGe eutectic.

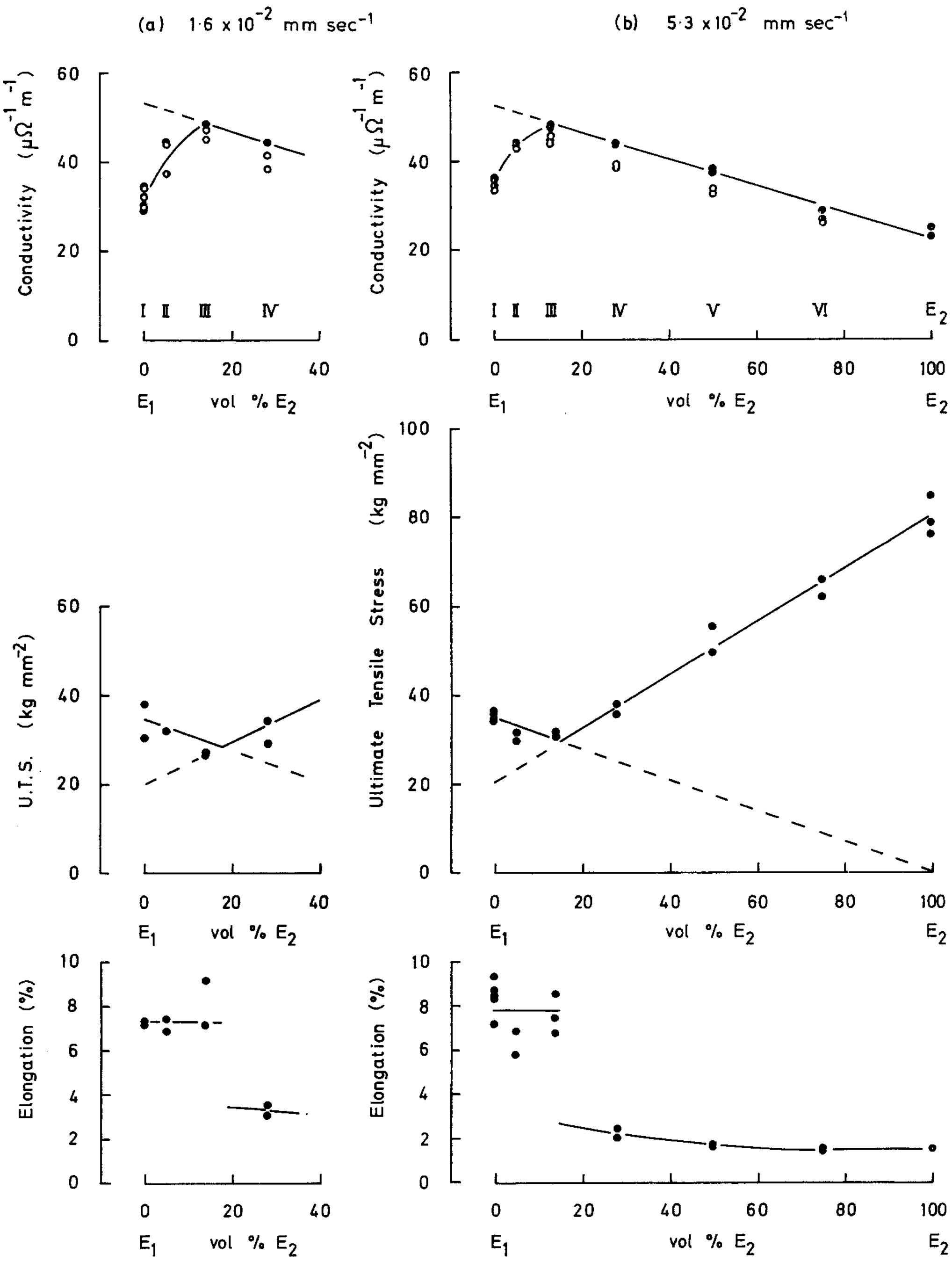


*Figure 8* The electrical conductivity, UTS and extension-to-fracture of heat-treated samples of alloys I-VI on the copper-CuZrGe to copper-$Cu_5Zr$ ($E_1$—$E_2$) tie-line after being grown at (a) 1.6, (b) 5.3 and (c) $16.0 \times 10^{-2}$ mm $sec^{-1}$. The conductivity before heat-treatment (open symbols) is also indicated (*figure continued on opposite page*).

objective of this study: namely the dependence of the tensile properties on volume fraction of $E_t$ – this latter because the $Cu_5Zr$ phase is the load carrier in both $E_2$ and $E_t$ and its volume fraction is about the same in them.

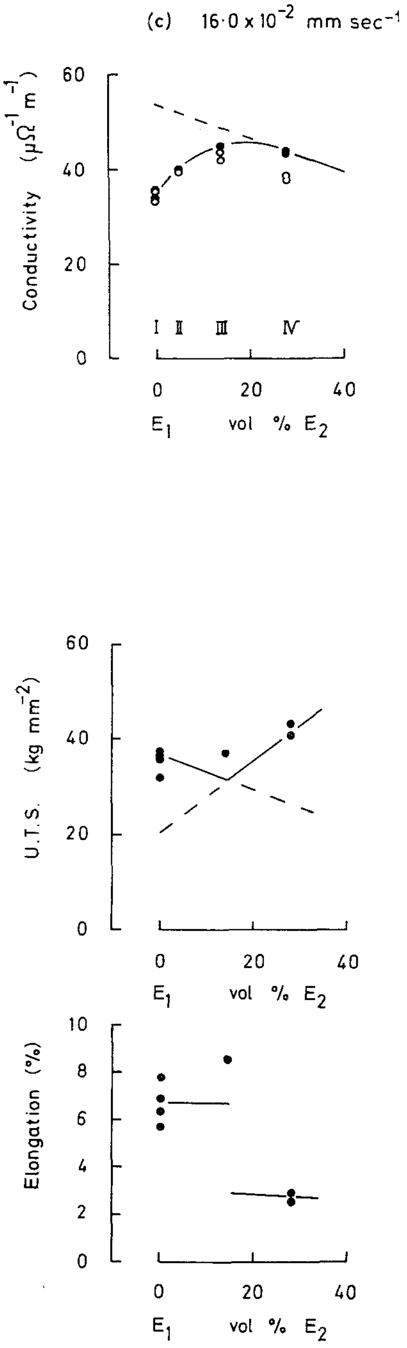


## 6. Properties of alloys on the $E_1$ — $E_2$ tie-line

Typical stress-strain curves of alloys on the $E_1$—$E_2$ tie-line are given in Fig. 5b. The change in ductility between alloys III and IV is quite marked.

The conductivity and tensile properties were only measured over the whole range of alloys I-VI in samples grown at one speed, namely $5.3 \times 10^{-2}$ mm sec$^{-1}$. The results are presented in Fig. 8b. The UTS and fracture strain extrapolate to the values found previously [5] for $E_2$, supporting the proposed proximity in phase space of $E_2$ and $E_t$, which permits the $Cu_5Zr$ in $E_t$ to be considered the major load carrier and the comparison with the $E_2$ data in Fig. 5, to be made.

The data obtained at the growth speeds of 1.6 and 16.0 mm sec$^{-1}$ over the limited composition range of alloys I-IV are given in Figs. 8a and c. They follow the same form as before. Following on from the discussion given below, the superposed curves are based on "law-of-mixtures" using the UTS of $E_2$ measured earlier [5] at the appropriate speed. The agreement is satisfactory.

The eutectic $E_1$ has a lower UTS and is relatively ductile as compared with $E_2$, which is stronger but fractures after far less extension. The system thus parallels the copper-tungsten case [3, 6] and the present tensile data do indeed follow a "law-of mixtures" relation as shown in Fig. 8b. The UTS is proportional to the volume fraction of the major load carrying phase and fracture is controlled by the failure strain of this phase. The parallel change in the extension to fracture is apparent in Figs. 5b and 8. It is interesting to note in passing that the shift in control from $E_1$ to $E_t$ occurs approximately when the volume fractions of CuZrGe and $Cu_5Zr$ (Fig. 1) are about the same, indicating that the UTS of these phases are similar. This shift in control, however, depends on the growth rate (Fig. 8a-c) and would be displaced towards $E_2$ if $E_1$ were cell-free.

The alloys are composites of two eutectics, both based on copper. Copper is thus being reinforced by two types of lamellae at the same time. That their effects are not additive is apparent in Fig. 8. In accord with the results from copper-tungsten, in $E_t$-rich alloys the more ductile phase – here $E_1$ – only contributes to the total UTS to the extent of the stress it is carrying when $E_t$ fractures and the sample fails. When $E_1$ is the major load-carrying component, $E_t$ fails first and weakens the structure. Thus, as a consequence of the difference in fracture strains, the two phases CuZrGe and $Cu_5Zr$ do not act in concert but indeed detract from one another.

The electrical conductivity of the alloys, both before and after heat-treatment, is included in Fig. 8. The form at high $E_1$ levels (alloys I-III) is the same as found in the copper-CuZrSi case (Fig. 2), the conductivity is improved by making the alloy zirconium-rich. As before, a further slight improvement results from heat-treatment. This effect is independent of heat-treatment time but depends only on the mode of cooling. As a function of $E_2$ level, the conductivity goes through a maximum value (Fig. 8b) then falls as the volume fraction of copper falls towards $E_2$. An alternative way of interpreting the data is: the observed conductivity approaches the value expected from the copper volume fraction in an asymptotic fashion in going from $E_1$ to $E_2$. This is assumed to result from a change in the solvus limit of the copper as the alloy composition is altered. It is interesting that the extrapolation of the data at high zirconium levels from VI through III back to the composition $E_1$ (Fig. 8b), yields a value of about 53 $\mu\Omega^{-1}$ $m^{-1}$ which is what would be expected if the copper in this eutectic contained no CuZrGe in solution.

Considering all the data in Fig. 8, the actual values of conductivity are better (at least in the $E_1$-rich alloys I-IV which were studied at different speeds) at lower growth rates, which confirms the structure-sensitivity found [5] in the earlier work on $E_2$.

## Acknowledgements

The authors wish to express their appreciation of the extensive metallography carried out by Mrs B. Höhn. They are also grateful to Dr P. J. Goodhew for making available the Quantimet facility.

## References

1. A. J. PERRY, *Mat. Sci. & Eng.* **11** (1973) 203.
2. K. DIES, "Kupfer und Kupferlegierungen in der Technik" (Springer Verlag, Berlin, 1967) p. 140.
3. A. KELLY and W. R. TYSON, *J. Mech. Phys. Solids* **13** (1965) 329.
4. J. NICKL and H. SPRENGER, *Naturwiss.* **54** (1967) 515.
5. A. J. PERRY, *J. Mater. Sci.* **8** (1973) 443.
6. D. L. MCDANELS, R. W. JECH, and J. W. WEETON, *Trans. AIME* **233** (1965) 636.
7. "Metals Handbook" 8th edn (ASM, Cleveland, Ohio, 1961) p. 1203.
8. A. J. PERRY and W. HUGI, *J. Inst. Met.* **100** (1972) 378.
9. M. J. SAARIVIRTA, *Trans. AIME* **218** (1960) 431.

Received 16 November and accepted 20 November 1972.